Thin film evolution equations from (evaporating) dewetting liquid layers to epitaxial growth

U. Thiele*†

Department of Mathematical Sciences, Loughborough University, Leicestershire LE11 3TU, UK

In the present contribution we review basic mathematical results for three physical systems involving self-organising solid or liquid films at solid surfaces. The films may undergo a structuring process by dewetting, evaporation/condensation or epitaxial growth, respectively. We highlight similarities and differences of the three systems based on the observation that in certain limits all of them may be described using models of similar form, i.e., time evolution equations for the film thickness profile. Those equations represent gradient dynamics characterized by mobility functions and an underlying energy functional.

Two basic steps of mathematical analysis are used to compare the different system. First, we discuss the linear stability of homogeneous steady states, i.e., flat films; and second the systematics of non-trivial steady states, i.e., drop/hole states for dewetting films and quantum dot states in epitaxial growth, respectively. Our aim is to illustrate that the underlying solution structure might be very complex as in the case of epitaxial growth but can be better understood when comparing to the much simpler results for the dewetting liquid film. We furthermore show that the numerical continuation techniques employed can shed some light on this structure in a more convenient way than time-stepping methods.

Finally we discuss that the usage of the employed general formulation does not only relate seemingly not related physical systems mathematically, but does as well allow to discuss model extensions in a more unified way.

The paper is published in: *J. Phys.-Cond. Mat.* **22**, 084019 (2010) and can be obtained at http://dx.doi.org/10.1088/0953-8984/22/8/084019

* homepage: http://www.uwethiele.de

†Electronic address: u.thiele@lboro.ac.uk

I. INTRODUCTION

Structure formation at interfaces and surfaces occurs widely in our natural and technological environment. The spectrum of related phenomena ranges from growing dendrites in solidification or crystallization to budding membranes in the biological cell. Technological processes based on or affected by interfacial structuring processes involve, for instance, the sputtering of solid surfaces (that may roughen), the usage of instabilities in the epitaxial growth of nano- or quantum-dots, the structuring of homogeneous liquid or elastic coating layers, the deposition of structured nano-particle assemblies employing instabilities, and heat-exchanger technology based on transfer enhancement by surface waves on falling liquid films. A selection is discussed in [1].

Part of the mentioned structuring processes can be modeled as an evolution in time of a surface profile. Models are normally based either on a stochastic microscopic discrete or a deterministic mesoscopic or macroscopic continuum approach. For an overview of methods for the modelling of (solid) nanostructures see [2]. Here, we focus on the continuum approach. There exists an important subset of systems that evolve towards an equilibrium state corresponding to an energetic minimum, i.e., normally these are relaxational systems without any external forcing.

A continuum description of relaxational systems can often be brought into the form of time evolution equation(s) for one or several conserved or non-conserved order parameter fields $\phi(\mathbf{x}, t)$ (cf. [3]). A non-conserved field might still follow in part a conserved dynamics. The dynamics is governed by the underlying energy functional $F[\phi]$. The simplest form for a time evolution of a purely dissipative system without any inertial hamiltonian dynamics corresponds to the gradient dynamics

$$\partial_t \phi \;=\; \nabla \cdot \left[M_{\mathrm{c}} \nabla \frac{\delta F}{\delta \phi} \right] \;-\; M_{\mathrm{nc}} \frac{\delta F}{\delta \phi} \tag{1}$$

with the $M_{\mathrm{c}}(\phi) \geq 0$ and $M_{\mathrm{nc}}(\phi) \geq 0$ being the mobility functions for the conserved and non-conserved part of the dynamics, respectively. Here and in the following ∂_t and ∂_x denote partial derivatives w.r.t. time and space, respectively.

A typical example is the Cahn-Hilliard equation describing the demixing of a binary mixture, i.e., a purely 'conserved dynamics' ($M_{\mathrm{nc}} = 0$) [3–5]. Another example is the Allen-Cahn equation describing, for instance, the dynamics of the Ising model in the continuum limit [3]. Multiplying Eq. (1) by $\delta F/\delta \phi$ and integrating one obtains after a partial integration

$$\frac{dF[\phi]}{dt} \;=\; -\int M_{\mathrm{c}} \left(\nabla \frac{\delta F}{\delta \phi} \right)^2 dV \;-\; \int M_{\mathrm{nc}} \left(\frac{\delta F}{\delta \phi} \right)^2 dV \leq 0 \tag{2}$$

confirming $F[\phi]$ to be a Lyapunov functional.

In the context of evolving surfaces or interfaces, such an equation appears in various contexts. We will discus here (i) film thickness equations for films of non-volatile and volatile liquids on solid substrates and (ii) surface profile equations for epitaxial growth.

Eq. (1) might describe the evolution of the surface profile of an evaporating or condensing thin liquid film on a solid substrate under the influence of capillarity and wettability. In this case, the function $\phi(\mathbf{x}, t)$ represents the film thickness profile and the functional $F[\phi]$ is given by

$$F[\phi] \;=\; \int \Big[\frac{\gamma}{2}(\nabla\phi)^2 + f(\phi) - \mu\phi\Big]\, dV \tag{3}$$

where γ is the liquid-gas surface tension and $f(\phi)$ is a local free energy, related to the disjoining pressure $\Pi(\phi)$ by $\Pi = -\partial_\phi f(\phi)$. The term $\mu\phi$ represents an overall energy bias towards the liquid or the gaseous state. It is the sole responsible for evaporation/condensation of flat 'bulk' films, i.e., films that are thick as compared to the range of the disjoining pressure. μ corresponds to a chemical potential. For details and specific choices for the disjoining pressure see, e.g., Refs. [6–11].

For Poiseuille flow in the film without slip at the substrate the mobility for the conserved part is $M_{\mathrm{c}} = \phi^3/3\eta$ where η is the dynamic viscosity. Several slip regimes might be accounted for by different choices for $M_{\mathrm{c}}(\phi)$ [12]. The mobility function for the non-conserved part is normally assumed to be a constant (see [13]). Note that there exists an ongoing discussion regarding the form of the non-conserved part of the dynamics (cf. e.g. [13–18]).

Eq. (1) with (3) is extensively studied in the conserved case, i.e., for non-volatile films ($M_{\mathrm{nc}} = 0$). It can easily be derived from the Navier-Stokes equations and appropriate boundary conditions at the substrate and the free surface employing a long-wave or lubrication approximation [9, 11]. Depending on the particular physical situation studied many different forms for the local energy function $f(\phi)$ are encountered. Beside 'proper' disjoining pressures that model effective molecular interactions between film and substrate (wettability) [6, 7, 10, 19–24] the equations may as well incorporate other pressures modelling, e.g., the influence of an electric field on a film of dielectric liquid in a capacitor [25–29] or films on homogeneously heated substrates that form structures due to a long-wave Marangoni instability [14, 30–34]. The latter is especially interesting because it represents a system that is kept permanently out of equilibrium but is nevertheless described by a gradient dynamics. Note that the situation is slightly different in a closed two-layer system [35] that can in two dimensions be described by Eq. (1) with an appropriate $F[\phi]$ but not in three

dimensions.

The above mentioned Cahn-Hilliard equation describing the conserved dynamics of demixing of a binary mixture corresponds to Eq. (1) and Eq. (3) with a constant $M_{\rm c}$, $M_{\rm nc} = 0$ and $f(\phi)$ being a symmetric double well potential. In consequence, many results obtained for the decomposition of a binary mixture have a counterpart in the dewetting of thin films and vice versa. The analogy was first noted by Mitlin [8] resulting in the notion of 'spinodal dewetting'. Note that there exist other choices for $f(\phi)$ and $M_{\rm c}$ in the Cahn-Hilliard equation [36, 37].

Equations of similar form may as well model the epitaxial evolution of surfaces of crystalline solids [2, 38–40]. We illustrate this employing one of the local models for Stransk-Krastanov growth found in the literature – namely a simplified 'glued wetting-layer model' (for details and derivation see refs. [40, eqs. 18-20] and [41]). The model assumes an isotropic wetting energy of the epitaxial film on the solid substrate, that is added to the (anisotropic) surface energy. Elastic stresses act through a destabilizing surface stiffness term. It is furthermore assumed that a given amount of material is deposited on the surface that then re-arranges in a process of self-organisation that might lead to the creation of nano- or quantum-dots, i.e., localized surface structures on the nanometre lengthscale. In the case of high-symmetry orientations of a crystal with cubic symmetry the evolution of the surface profile $\phi(\mathbf{x}, t)$ is described by Eq. (1) when using small-slope approximation. As the amount of material is fixed only the conserved part contributes, i.e., $M_{\rm c} > 0$ and $M_{\rm nc} = 0$. The model in [40] employs a constant mobility $M_{\rm c}$ (corresponding to a constant surface diffusion coefficient). Non-constant mobilities might as well be used. Note that a fourth-order kinematic term is omitted in the evolution equation as it can lead to artifacts if the slope of the interface is large (inside the small slope approximation, for details see [41]). The free energy functional is

$$F[\phi] \;=\; \int \Big[-\frac{\sigma}{2}(\nabla\phi)^2 + \frac{\nu}{2}(\Delta\phi)^2 + \frac{a}{12}(\nabla\phi)^4 + f(\phi) - \mu\phi \Big]\, dV \tag{4}$$

where $\sigma > 0$ is the destabilizing surface stiffness resulting from elastic stresses, $\nu > 0$ represents the energetic cost of corners and edges, and a quantifies the slope-dependent anisotropic surface energy (note that we fixed the b of [40] as $b = a/3$ to simplify the equation for the present purpose of comparison). The local free energy $f(\phi) = \int W_0(\phi) d\phi$ results from the wetting interaction. Thereby $W_0 = -w(\phi/\delta)^{-\alpha_w} \exp(-\phi/\delta)$ where δ is a characteristic wetting length, the positive w and α_w characterize the strength and singularity of the underlying interactions. The singularity ensures the stability of the stable monolayer between surface elevations in Stranski-Krastanov

growth. Without wetting interactions the epitaxial film would show Volmer-Weber growth, i.e., growth would occur in separated islands not connected by a wetting layer. Note that we here add the last term to eq. 4 where μ is the chemical potential. It does not affect the evolution equation when $M_{\rm nc} = 0$. Related (in part non-local) equations are employed in Refs. [2, 42–46].

If vapour deposition is used to deposit the epitaxial layer it is to expect that equation (1) with (4) and $M_{\rm nc} > 0$ well describes the process. We are, however, not aware of such an approach in the literature. Actually, for large chemical potential μ as compared to the other terms in F (Eq. (4)) one can even use the system to describe the evolution under vertical deposition of material. The constant $M_{\rm nc}\mu$ does then corresponds to the constant deposition rate in other models (V in [38]).

Although the overall form of the equation is identical for the various problems introduced above, the specific physics is very different. However, still one can employ the same set of techniques to analyse the various models. Normally, one uses (i) a linear stability analysis of homogeneous steady states, i.e. flat films to determine the stability of the system and typical length scales that will dominate the short-time evolution in case the homogeneous state is unstable. (ii) Depending on the properties of the dispersion relation obtained in the linear stability analysis one might be able to analytically study stable and unstable steady state solutions and their stability in the weakly non-linear regime. This is, however often not possible. (iii) In the strongly non-linear regime steady states and their stability might still be obtained, e.g., using continuation techniques [47, 48]. These are readily available for two-dimensional systems that can be expressed as ordinary differential equations [49]. Recently, they were also introduced for the full three-dimensional problem, in particular for Eq. (1) with $M_{\rm nc} = 0$ and (3) [50]. Note, that variational methods are apt to obtain the steady states directly from the functional F, but are not suitable to discuss the stability of the steady states as this involves dynamic aspects. Many groups prefer to 'skip' step (iii) and rather directly (iv) simulate the evolution equation in time using advanced numerical techniques (spectral, pseudo-spectral, or semi-implicite).

We remark here that other types of continuum description exist for all the mentioned systems. Whereas here we focus on evolution equations for surface or interface profiles, another class of models describes interface evolution using phase fields [51]. See, for instance, for dewetting and liquid films/drops in general Ref. [10] and for epitaxial growth Ref. [2, 43, 52]. We do entirely exclude from our consideration the vast literature on discrete stochastic models that exist for dewetting/evaporation processes (e.g., [53–55] as well as for surface growth (for reviews see, e.g., [56, 57]).

In the following, we restrict ourselfes to two-dimensional physical situations described by film thickness profiles $\phi(x,t)$ that depend on one spatial coordinate only. The drops or quantum-dots in 2d will actually refer to liquid ridges or quantum-wires in 3d, respectively. We will perform a basic analysis of linear stability and steady states 'in parallel' for a dewetting liquid film on a solid substrate (Section II), a dewetting evaporating/condensing liquid film on a solid substrate (Section III), and the epitaxial structuring of a solid film (Section IV). Note that we only review steps (i) and (iii) of the above introduced scheme that sketches a more complete analysis of the system behaviour. The next step would be to use advanced numerical techniques to simulate the evolution of the films in time for two- and three-dimensional physical settings. It involves a rather large number of techniques and groups and we would like to refer the reader to the individual publications cited in the respective sections below.

Before we start we would like to point out the relevance of stable and unstable steady state solutions for systems that evolve in time. Most steady state solutions are either not linearly stable or do not correspond to the global energetical minimum that the system will finally approach. Such solutions are normally not well appreciated in the literature as they are not present 'in equilibrium'. They are, however, often present for a long time in the course of the time evolution and due to their character as saddles in function space they do often 'structure' the evolution towards equilibrium. Their stability properties (i.e., growth and relaxation rates) determine time-scales for important steps of the dynamics. and as important transients in experiments of finite duration they might actually even get 'frozen in' or 'dried in' as, e.g., in the dewetting of thin polymer films [58, 59] or suspensions [60, 61], respectively. In this connection, coarsening, is a particularly interesting issue as in its course the system 'passes through' an infinite number of steady state solutions that are stable when taking their typical size as reference size, but are unstable with respect to modes on larger lengthscales, i.e. with respect to coarsening. One could say the individual solutions do first 'attract a time-evolution' and then 'expel it' along the single unstable direction (corresponding to coarsening).

II. DEWETTING

A dewetting film of non-volatile liquid on a solid substrate is modelled by Eqs. (1) and (3) with $M_{\rm nc} = 0$ [8, 9, 11]. The local energy $f(\phi)$ corresponds to a disjoining pressure $\Pi(\phi) = -\partial_\phi f(\phi)$ [6, 7, 19]. Various functional forms are used for $f(\phi)$. The particular choice is, however, not very

relevant for the qualitative behaviour of the system. The latter only depends on the number and relative depth/height of the extrema of $f(\phi)-\mu\phi$. We choose here $f(\phi) = -\kappa[1/(2\phi^2)-b^3/(5\phi^5)]$ as derived by Pismen from a modified Lennard-Jones potential with hard-core repulsion [62–64]. The resulting $f(\phi)$ has only one minimum at a finite $\phi_{\rm precursor} = b$. The parameter κ corresponds to a typical energy scale. With the chosen signs the first term corresponds to a destabilizing long-range van der Waals interaction (i.e., κ is proportional to a Hamacker constant) whereas the second one represents a short-range stabilizing interaction. In consequence, the model may describe drops of a partially wetting liquid in co-existence with a precursor film of thickness b. In the following we scale ϕ by the precursor film thickness, i.e., we fix $b = 1$.

If there existed a second minimum at larger finite thickness it would correspond to a critical height for the transition between spherical-cap-like drops and pancake-like drops (e.g., the capillary length when gravity is included) [6, 65]. For a selection of other pressure terms see, e.g. [6, 8, 10, 59, 60, 66–70].

Inspecting Eq. (1) with $M_{\rm nc} = 0$ one notes that any flat film (thickness $\phi = \phi_0$) corresponds to a steady state solution of the system. However, those films might not be stable: We linearize the system about the flat film employing harmonic modes, i.e., $\phi(x,t) = \phi_0 + \epsilon\, \exp(\beta t + ikx)$ where $\epsilon \ll 1$ is the smallness parameter, β the growth rate of the harmonic mode of wavenumber k. Entering this ansatz in Eq. (1) with (3) gives the dispersion relation

$$\beta(k) \;=\; -M_{\rm c}^0\, \gamma\, k^2\, (k^2 - k_c^2), \tag{5}$$

where $M_{\rm c}^0 = M_{\rm c}(\phi = \phi_0)$. The critical wavenumber is given by $k_c = \sqrt{-\partial_{\phi\phi} f|_{\phi=\phi_0}/\gamma}$. For $\partial_{\phi\phi} f|_{\phi=\phi_0} < 0$ the film is linearly unstable for $0 < k < k_c$. The most dangerous instability mode, i.e., fastest growing mode has $k_{\rm max} = k_c/\sqrt{2}$ and $\beta_{\rm max} = M_{\rm c}^0 \gamma k_c^4/4$. The onset of the instability occurs at $\partial_{\phi\phi} f|_{\phi=\phi_0} = 0$ with $k_c^{\rm onset} = 0$, i.e., it is a long-wave instability. Note that mass conservation implies $\beta(k = 0) = 0$. Examples of dispersion relations above and below the instability treshhold are given in Fig. 1.

Steady film thickness profiles are obtained by solving Eq. (1) with $\partial_t \phi = 0$. Note that in the present setting this corresponds to $\delta F/\delta\phi = 0$ because the first integration constant (when integrating Eq. 1) is zero as we look at systems without large-scale meanflow. The whole solution structure might be mapped out in parameter space employing continuation techniques using analytically or numerically known solutions to start the continuation [11, 47–49]. Many parameters might be used as main continuation parameter, e.g., period or domain size, film thickness, or any

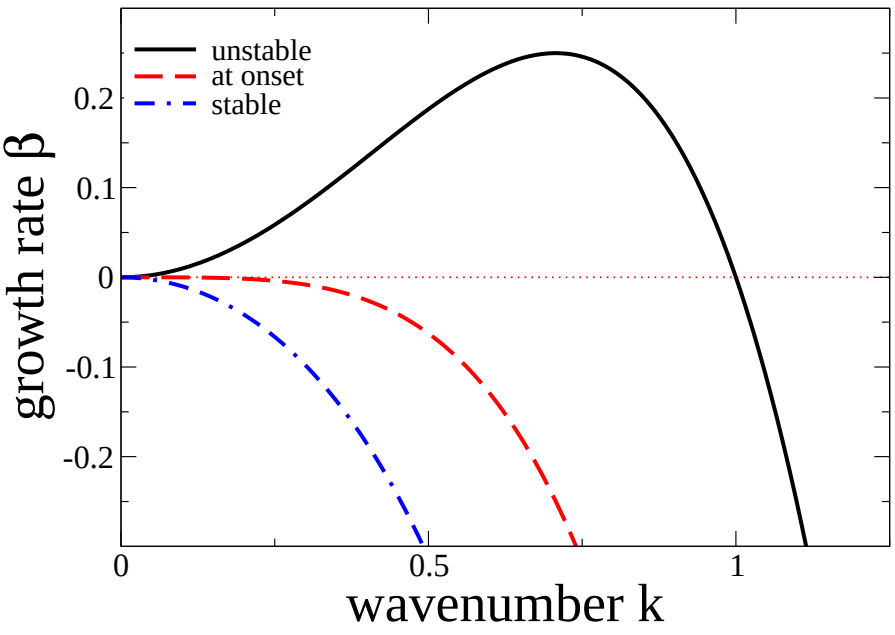

FIG. 1: Dispersion relations for the instability of a flat liquid film w.r.t. surface modulations resulting in dewetting and the evolution of patterns of droplets. Shown is a stable and an unstable case in the generic form $\beta = -k^2(k^2 - k_c^2)$, i.e., the growth rate β is scaled by $M_c^0\,\gamma$. The wave number is given in units of k_c.

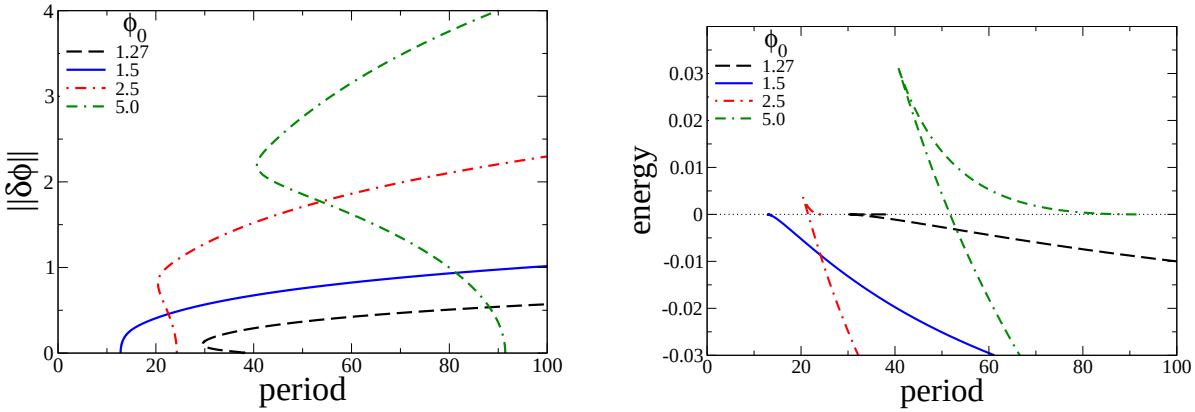

FIG. 2: Shown are characteristics of families of steady one-dimensional droplet structures arising in dewetting of a non-volatile liquid using a simple disjoining pressure. The left panel gives the L_2-norm $||\delta\phi||$ and the right one the energy F (Eq. (3)) per length. The legends give the corresponding mean film thicknesses. The families are obtained using continuation techniques. Note that the solutions are unstable w.r.t. coarsening.

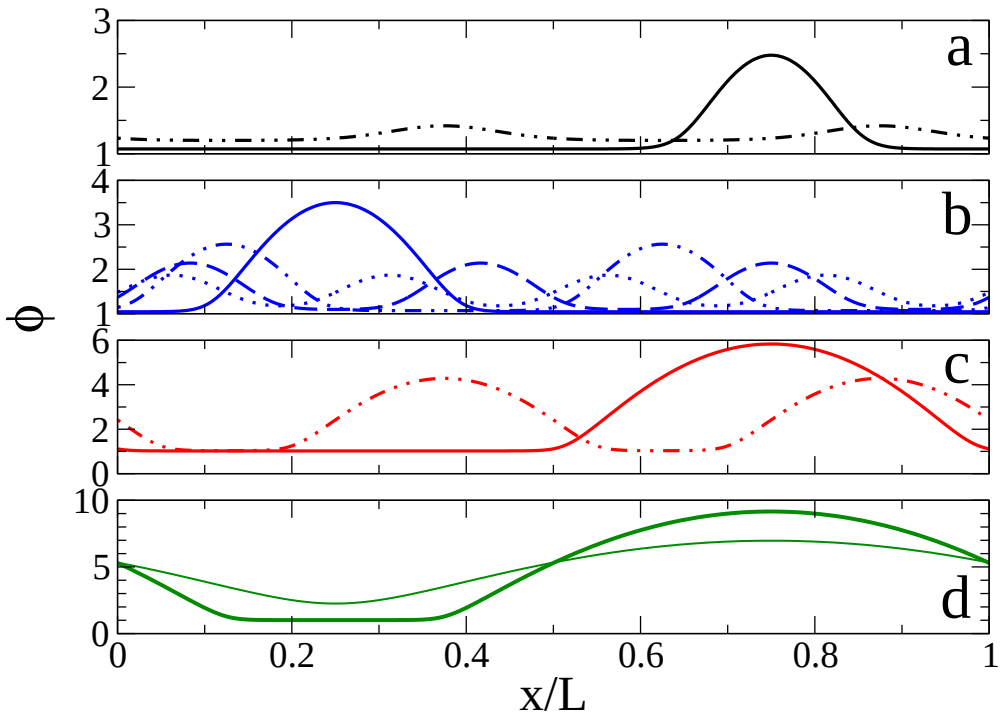

FIG. 3: Shown are examples of film thickness profiles for the various branches presented in Fig. 2. Mean thicknesses $\bar{\phi}$ are (a) 1.27, (b) 1.5, (c) 2.5, and (d) 5.0. The system size is $L = 60$ in all cases. Given are profiles from the following branches: $n = 1$ (solid lines), $n = 2$ (dot-dashed lines), $n = 3$ (dashed line), and $n = 4$ (dotted line). The thin line in (d) corresponds to a nucleation solution. For given L only the $n = 1$ profiles are stable w.r.t. coarsening.

parameter of the energy. Here we only use system size. For a more detailed explanation of the continuation procedure for thin film equations see the Appendices of [71, 72].

For a linearly unstable film a one parameter family of periodic film profiles bifurcates from the flat film at wavenumber k_c as illustrated in Fig. 2. At the bifurcation point a steady harmonically modulated surface profile exists with a period of $2\pi/k_c$ and an infinitesimally small amplitude. Using period as main continuation parameter the whole family of periodic solutions can be obtained. A selection of resulting film thickness profiles is given in Fig. 3. We characterize solutions by their norm $||\delta\phi|| = [(1/L)\int_0^L(\phi(x)-\phi_0)^2dx]^{1/2}$ and energy per length $E = (1/L)\int_0^L F[\phi]dx$. Note that mass conservation advises us to directly compare only profiles of identical mean film thickness. This is ensured by μ acting as a Lagrange multiplier. In consequence, μ changes along the individual branches in such a way that the mean of $\phi(x)$ is kept fixed.

The resulting branches might bifurcate from the trivial solution supercritically, i.e., they bifur-

cate towards the region of the linearly unstable flat film (forward towards larger periods; see, e.g., in Fig. 2 curve for $\phi_0 = 1.5$). Or the branch bifurcates subcritically, i.e., it emerges towards the region of the linearly stable flat film (backward towards smaller periods; see, e.g., in Fig. 2 curves for $\phi_0 = 1.27, 2.5$, or 5.0). The location of the border between sub- and supercritical behaviour can be determined employing a weakly nonlinear analysis and can be expressed as an algebraic condition for the 2nd, 3rd and 4th derivative of $f(\phi)$ [73].

In the case of the subcritical bifurcation, the subcritical branch (i.e., between the bifurcation and the saddle-node bifurcation where it 'folds back' towards larger periods) consists of unstable, nucleation solutions that aquire an importance for the rupture process of the film if the system is noisy or 'dirty': Note that for the chosen potential $f(\phi)$ there exist no metastable films. However, one may distinguish two thickness ranges within the linearly unstable range: (i) the linearly unstable modes are fast and will dominate the time evolution even in the presence of defects (finite size perturbations); (ii) the linear modes are slow, and defects – if there are any present – will dominate the time evolution. The distinction is related to the existence of the subcritical branch of unstable solutions. They correspond to nucleation or threshold solutions as they have to be overcome to break the film into drops smaller than the critical wavelength of the linear instability. As they are saddles in function space they can 'organize' the evolution of defect-ridden thin films by offering a fast track to film rupture. This allows to determine a typical time for nucleation events even inside the linear unstable regime and finally to distinguish the nucleation-dominated and instability-dominated behaviour of linearly unstable thin films [24, 74]. A detailed account and comparison to the results of [75] is found in Ref. [76]. Note that similar ideas have since been applied to the break-up of liquid ribbons [77]. Recently we also performed a more detailed analysis for a three-dimensional systems [50, 78].

For unstable flat films of thicknesses ϕ_0 the respective branches of solutions bifurcating at $L_c = 2\pi/k_c$ shown in Fig. 2 are only the first of an respective infinite number of primary solution branches. These bifurcate at domain sizes $L_{cn} = 2\pi n/k_c$, $n = 1, 2, \ldots$. The branch bifurcating at L_{cn} consist of the $n = 1$ branch 'stretched in L' by a factor n. The actual thickness profiles of the n branch consist of n identical drops. This representation of the periodic solutions in dependence of domain size might seem pointless for the present problem. The reason is that the different branches are entirely decoupled. As the situation changes strongly when either looking at other energy functionals (see below Section IV), or when breaking the reflection or translational symmetry of the system (by including a lateral driving force [34, 65, 79], substrate heterogeneity [71], or lateral

boundary conditions [80]) it is, however, useful to introduce the various branches here.

The monotonous decrease of energy (on the low energy branch) with system size indicates that the system tends to coarse towards larger and larger structure size. The steady solutions on the 'stable' branches (the branches of drop solutions that continue towards infinite period) are stable when looked at in a domain of the size of their period, but unstable on larger domains, i.e., they are saddles in function space that form the 'stepping stones' of the coarsening process: They first 'attract the time-evolution' and then 'expel it' along the only unstable direction (corresponding to coarsening). The coarsening behaviour for a dewetting film is discussed in more detail in Refs. [81–84]. Related results for the Cahn-Hilliard equation are discussed, e.g., in Refs. [3, 85, 86].

Note that results on the nonlinear stability of flat films and the related steady state solutions on branches not connected to the trivial flat film solutions are not discussed here (but see [11, 34, 76]). For discussions of the evolution in time of dewetting films in two- and three-dimensional settings we refer the reader to Refs. [9, 22, 27, 32, 33, 50, 75, 77, 87, 88]. Note finally that continuation may not only be used to obtain families of steady or stationary profiles [65, 70, 72, 73, 89], but as well to track their stability and bifurcations [34, 90–92].

III. EVAPORATION

When including evaporation in the presently studied framework one uses Eq. (1) with the energy functional (3) and $M_{\rm nc} \neq 0$. One notes that unlike the case without evaporation flat films of arbitrary thickness $\phi = \phi_0$ do not correspond to a steady state solution of the system any more. However, steady flat film solutions still exist when wettability and evaporation balance. For a given chemical potential the corresponding steady thicknesses are given by

$$\partial_\phi f|_{\phi=\phi_0} = \mu, \tag{6}$$

i.e., for the disjoining pressure used here $\phi_0 = [\kappa(1 \pm (1 - 4b^3\mu/\kappa))^{1/2}/2\mu]^{1/3}$. For condensation ($\mu > 0$) two such equilibria exist if $\mu < \kappa/4b^3$ whereas for evaporation ($\mu < 0$) only one thickness exists. Note that this might be different for qualitatively different disjoining pressures like the one used in [13]. As above the steady films might be unstable.

We linearize Eq. (1) with (3) about the flat film of thickness ϕ_0 given by Eq. (6) employing

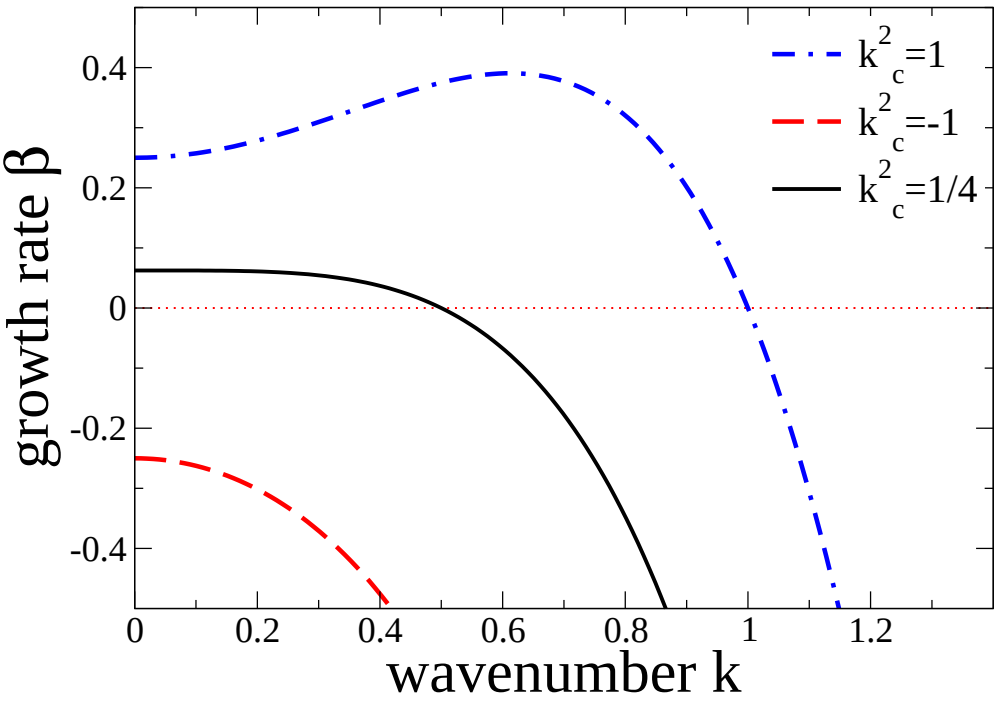

FIG. 4: Dispersion relations for the instability of a flat volatile liquid film w.r.t. surface modulations resulting in the evolution of a pattern of droplets. Shown are three qualitatively different cases in the generic form $\beta = -(k^2 + M^0_{\rm nc}/M^0_{\rm c})\,(k^2 - k_c^2)$, i.e., we fix $\gamma M^0_{\rm c} = 1$. We furthermore choose $M^0_{\rm nc}/M^0_{\rm c} = 1/4$.

harmonic modes as above to obtain the dispersion relation

$$\beta(k) \;=\; -M^0_{\rm c}\,\gamma\left(k^2 + \frac{M^0_{\rm nc}}{M^0_{\rm c}}\right)\,(k^2 - k_c^2) \tag{7}$$

where $M^0_{\rm nc} = M_{\rm nc}(\phi = \phi_0)$, $M^0_{\rm c} = M_{\rm c}(\phi = \phi_0)$, and $k_c = \sqrt{-\partial_{\phi\phi} f|_{\phi=\phi_0}/\gamma}$ as without evaporation. As the expression in the first parenthesis is always positive the film is linearly unstable for $\partial_{\phi\phi} f|_{\phi=\phi_0} < 0$ in the wave number range $0 < k < k_c$. The most dangerous instability mode occurs for $k_{\rm max} = \sqrt{(k_c^2 - M^0_{\rm nc}/M^0_{\rm c})/2}$ with $\beta_{\rm max} = M^0_{\rm c}\,\gamma(M^0_{\rm nc}/M^0_{\rm c} + k_c^2)^2/4$ if the expression under the square root is positive. Otherwise the mode with $k = 0$ grows fastest ($\beta(k = 0) = M^0_{\rm nc} k_c^2$).

The onset of the instability occurs at $\partial_{\phi\phi} f|_{\phi=\phi_0} = 0$ with $k_c^{\rm onset} = 0$, i.e., it is a long-wave instability. Qualitatively different examples of dispersion relations above and below the instability treshold are given in Fig. 4.

As above steady thickness profiles are obtained by setting $\partial_t \phi = 0$ in Eq. (1). For a linearly unstable film a one parameter family of profiles bifurcates from the flat film at k_c as illustrated in the four panels of Fig. 5. In contrast to the case without evaporation/condensation here the mean film thickness changes along the branches whereas the imposed chemical potential remains

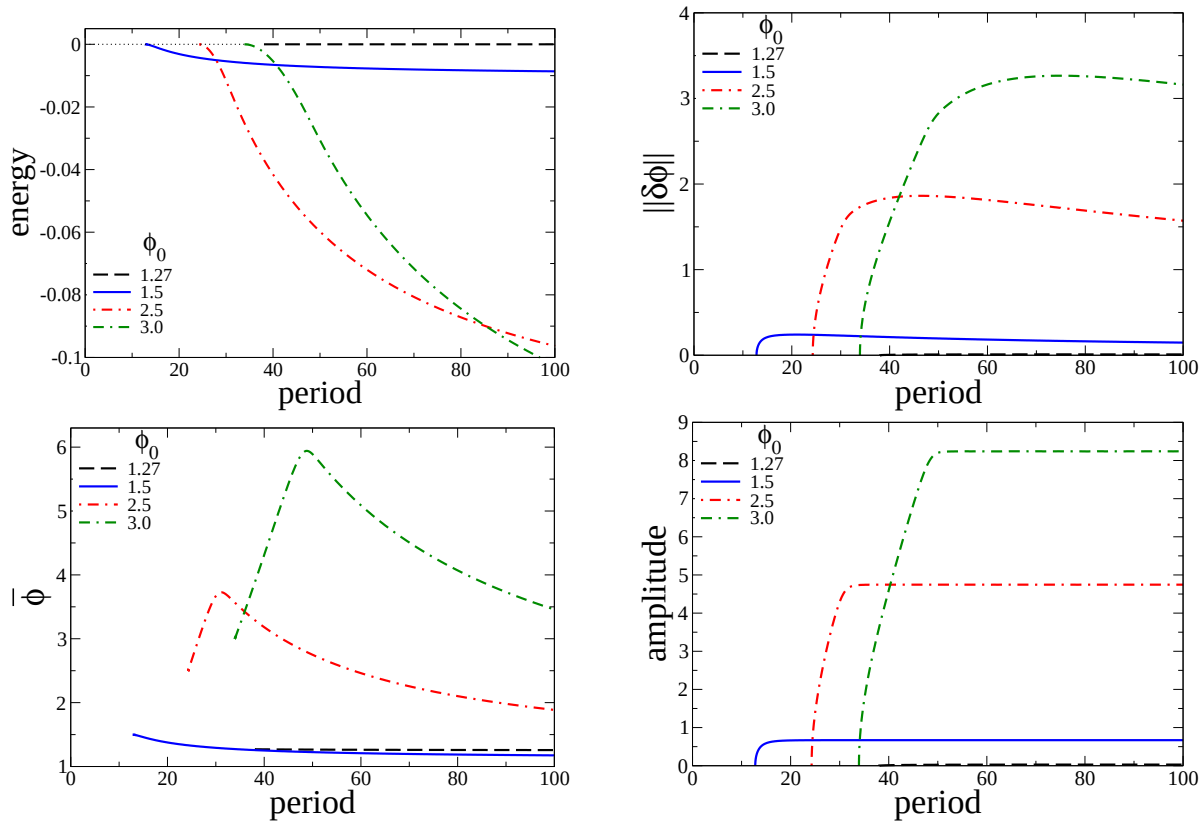

FIG. 5: Shown are characteristics of families of steady one-dimensional droplet structures arising in dewetting of a volatile liquid using a simple disjoining pressure. From top left to bottom right the panels give the L_2-norm, the energy F (Eq. (3)) per length, the mean film thickness $\bar{\phi}$, and the droplet amplitude. The legends give the corresponding mean film thicknesses for the flat film ϕ_0 at the identical chmicalpotential μ. The families are obtained using continuation techniques. Note that the solutions are unstable w.r.t. coarsening.

constant. A selection of film thickness profiles is given in Fig. 6.

Most notably the resulting branches always bifurcate supercritically from the trivial solution. The results furthermore indicate that there is no metastable film thickness range at all, implying that nucleation does not play any role for a condensing/evaporating film described by the present disjoining pressure. This, however, needs a deeper analysis in the future including a comparison of the behaviour for different pressure terms. Remarkably, the amplitude (droplet height) approaches a limiting value for a domain size of about $3L_c/2$. As the energy monotonously decreases with domain size we expect these solutions to be unstable w.r.t. coarsening as the droplet pattern in the non-volatile case. Note finally, that everything discussed above for non-volatile films regarding

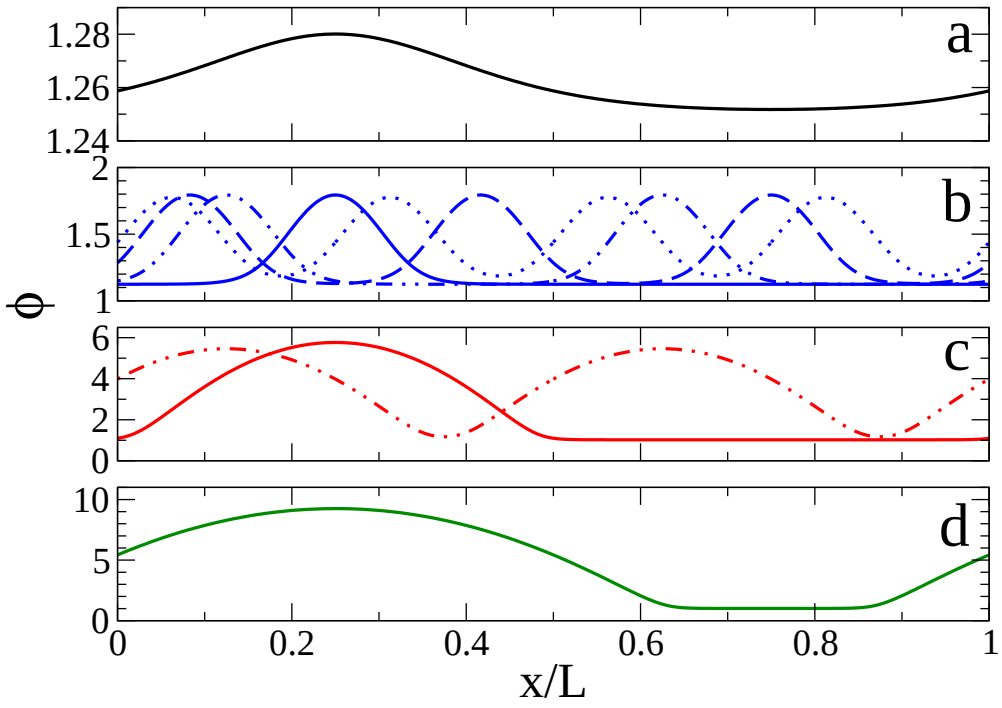

FIG. 6: Shown are examples of film thickness profiles for the various branches presented in Fig. 5. Mean thicknesses $\bar{\phi}$ are (a) 1.27, (b) 1.5, (c) 2.5, and (d) 3.0. The system size is $L = 60$ in all cases. Given are profiles from the following branches: $n = 1$ (solid lines), $n = 2$ (dot-dashed lines), $n = 3$ (dashed line), and $n = 4$ (dotted line).

the infinite number of primary solution branches as well applies to the branches shown in Fig. 5.

After the short analysis of the the volatile and non-volatile thin liquid film system we next focus on a thin film equation that describes the evolution of a solid film.

IV. EPITAXIAL GROWTH

The final example is a thin film model for the epitaxial evolution of surfaces of crystalline solids for a fixed ammount of deposited material that is illustrated here employing a simplified 'glued wetting-layer model' [40]. The evolution equation (1) describes such a system when combined with the energy functional (4) and $M_{\rm nc} = 0$. As in the case of the non-volatile liquid film material is conserved and any flat film of thickness $\phi = \phi_0$ corresponds to a steady state solution of the system.

As those trivial steady states might be unstable we perform a linear stability analysis along the

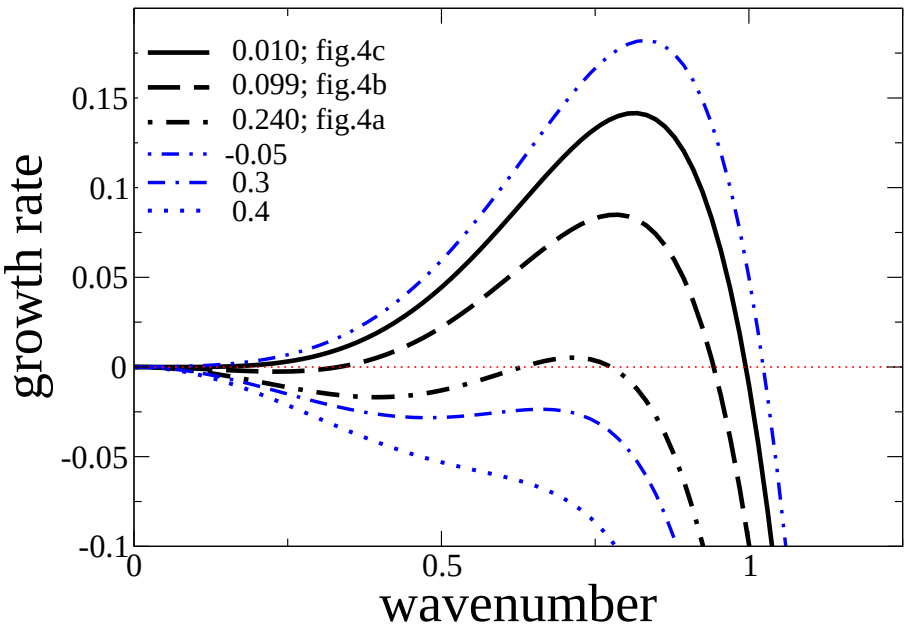

FIG. 7: Dispersion relations for the instability of a flat epitaxial film w.r.t. surface modulations resulting in the growth of quantum dots. Used is the simplest model proposed in Ref. [40]. The legend gives the dimensionless value of $\partial_\phi f$ at ϕ_0. Starting with the lowest one the three bold curves correspond to the cases studied in Figs. 4(a), (b) and (c) of [40].

lines of the previous sections and obtain the dispersion relation

$$\beta(k) \;=\; -M_c^0 \nu \; k^2 \left(k^2 - k_{c1}^2\right) \; \left(k^2 - k_{c2}^2\right) \tag{8}$$

with

$$k_{c1/c2} = \sqrt{\frac{\sigma}{2\nu}\left(1 \pm \sqrt{1 - \frac{4\nu\,\partial_{\phi\phi} f|_{\phi=\phi_0}}{\sigma^2}}\right)} \tag{9}$$

The film is linearly unstable for $\partial_{\phi\phi} f|_{\phi=\phi_0} < \sigma^2/4\nu$ in the wave number range $k_{c1} < k < k_{c2}$. The fastest growing mode has the wavenumber $k_{\max} = (\sigma/3\nu)^{1/2}\sqrt{1+\sqrt{1-3\nu\partial_{\phi\phi} f|_{\phi=\phi_0}/\sigma^2}}$. For values of $\partial_{\phi\phi} f|_{\phi=\phi_0} < 0$ one of the two critical wavenumbers becomes imaginary, i.e., the film is then unstable for $0 < k < k_{c2}$. Note that the onset of the instability occurs at $\partial_{\phi\phi} f|_{\phi=\phi_0} = \sigma^2/4\nu$ with $k_c^{\rm onset} = \sqrt{\sigma/2\nu}$, i.e., it is a short-wave instability. Qualitatively different examples of actual dispersion curves above and below the instability treshold are given in Fig. 7.

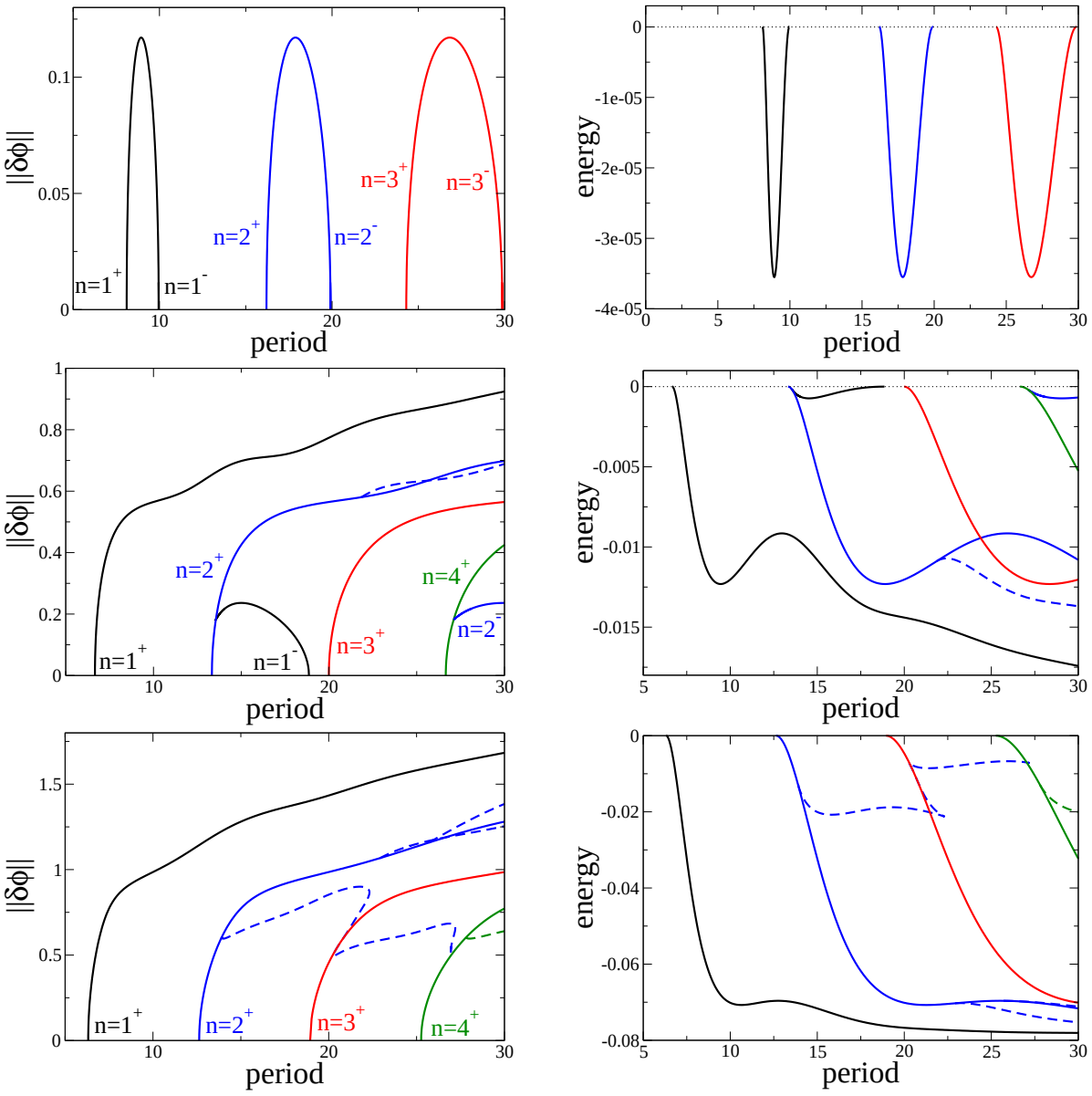

FIG. 8: Shown are characteristics of families of steady one-dimensional surface structures (quantum dots) arising in epitaxial growth using the simplest model proposed in Ref. [40]. The panels in the left column give the L_2-norm and the ones in the right column the energy F (Eq. (4)) per length. Parameter values correspond to (top row) Fig. 4(a), (middle row) Fig. 4(b), and (bottom row) Fig. 4(c) of [40]. From top to bottom the non-dimensional wetting interaction increases leading to more intricate behaviour. The families are obtained using continuation techniques.

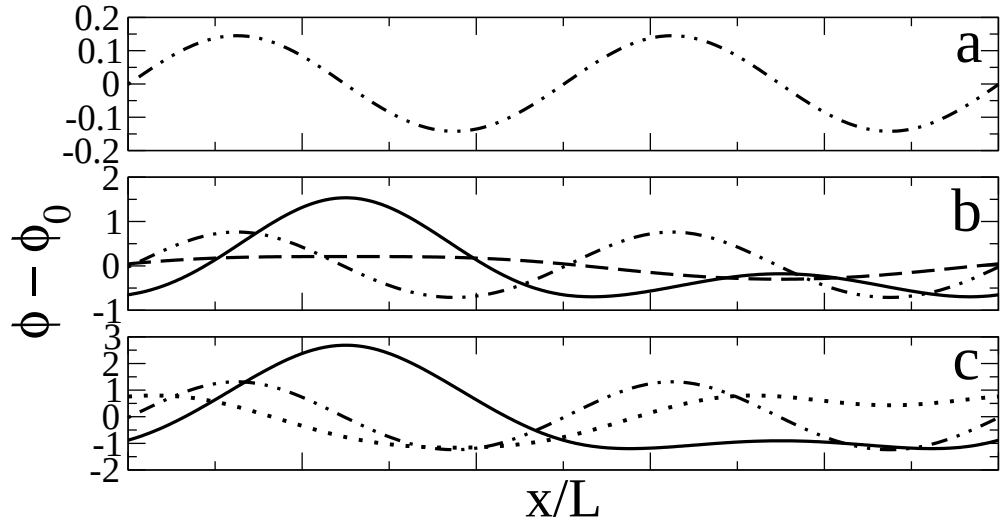

FIG. 9: Shown are examples of film thickness profiles ($\phi - phi_0$) for the various branches presented in Fig. 8. The parameters correspond to (a) the top row, (b) the middle row, and (c) the botom row of Fig. 8. The chosen system size is $L = 17$ in all cases. Given are profiles from the $n = 1^+$ branch (solid lines), the $n = 2^+$ branch (dot-dashed lines), the $n = 1^-$ branch (dashed line in (b)), and the first side branch of the $n = 2^+$ branch (dotted line in (c)) as defined in Fig. 8. Mean film thicknesses is $\phi_0 = 1.75$.

As in the other two cases steady thickness profiles are obtained by setting $\partial_t \phi = 0$ in Eq. (1). Here they do not represent profiles of liquid droplets, but profiles of solid quantum- or nanodots. Due to the higher order terms in the energy (4) as compared to the functional (3) studied up to now, the dispersion curves (Fig. 7) are qualitatively quite different from the ones for dewetting (Fig. 1). In consequence we expect a rather different picture for the steady state solutions as well. At the parameter values allowing for two critical wavenumbers k_{c1} and k_{c2}, i.e. for $\partial_{\phi\phi} f|_{\phi=\phi_0} > 0$, one finds two bifurcations from the trivial solutions at domain sizes $2\pi/k_{c1}$ and $2\pi/k_{c2}$, respectively. Near onset one expects the two emerging branches to interconnect, as at onset the solution space should change only locally. Further above onset the behaviour might, however, be dramatically different. The two branches bifurcating at $2\pi/k_{c1}$ and $2\pi/k_{c2}$ are the first of two infinite series of primary solution branches that bifurcate at respective domain sizes $L_{c1n} = 2\pi n/k_{c1}$ and $L_{c2n} = 2\pi n/k_{c2}$ with $n = 1, 2, \ldots$. This consideration is of importance here, as the various primary branches may actually couple.

We illustrate the solution structure in Fig. 8 using parameter values as in Fig. 4 of Ref. [40]. Shown are the norm (left column) and energy (right column) of the solutions on the various branches for three (positive) values of the strength of the wetting interaction. A selection of film

thickness profiles is given in Fig. 9. As the strength of the wetting interaction decreases the system gets deeper into the unstable regime and the behaviour becomes more intricate. In the upper row of Fig. 8 we are slightly above onset and the two $n = 1$ branches that emerge at the two zero crossings of the dispersion relation actually connect as expected. They are well separated from the branches with $n > 1$. Single-quantum-dot ($n = 1$) solutions only exist for a small range of periods $L_{c1} < L < L_{c2}$, i.e., the system is not able to undergo any coarsening. This corresponds well to the results obtained in [40] using weakly nonlinear analysis and integration in time. In the following we will call the branch emerging at iL_{c1} [iL_{c2}] the left [right] $n = i$ branch.

The picture changes, however, further above onset, i.e., when decreasing the wetting interactons (middle row of Fig. 8). The two $n = 1$ branches do not interconnect any more. Actually, the left $n = 1$ branch continues towards $L = \infty$ without any side branches. The left $n = 2$ branch may change its stability with respect to coarsening with increasing domain size. Every time it changes stability a secondary branch bifurcates in a period doubling bifurcation rather similar to the scenario described for driven liquid films on inlined plates [34]. The right $n = 1$ branch connects via one of the branching points to the left $n = 2$ branch. The behaviour becomes increasingly involved for higher branch numbers.

Decreasing the wetting interaction even more brings the system further above threshhold (bottom row of Fig. 8). As k_{c1} becomes quite small the right $n = 1$ branch bifurcates at very large domain sizes. However, the first secondary branch of the left $n = 2$ branch now split up into various pieces that connect different left branches via secondary bifurcations.

We will at present not go deeper into the analysis. In particular no proper stability analysis for the steady states is done here and as above for the dewetting system time evolution is not touched. Simulations can be found, for instance, in Refs. [2, 40, 42, 44–46]. Note that the results on stability sketched in the previous paragraph are infered from the structure of the bifurcation diagrams alone. They need to be scrutinized in detail as they are very important for the coarsening behaviour. The non-monotonous dependence of energy on system size in Fig. 8 indicates that coarsening will depend on structure length in a non-trivial way. The long-time corsening for epitaxial growth is discussed, e.g., in Refs. [93–95].

The results presented for the glued wetting-layer model indicate that our knowledge about epitaxial growth would benefit from a more detailed analysis that maps out the steady solutions and their stability systematically for the various models proposed in the literature. Numerical techniques are available to do this not only for two-dimensional but as well for three-dimensional

systems [50].

V. CONCLUSION

In the present contribution we have applied a basic mathematical analysis to three different physical systems involving solid and liquid films at solid surfaces that may undergo a structuring process by dewetting, evaporation/condensation or epitaxial growth, respectively. The aim has been to highlight similarities and differences of the three systems based on the observation that all of them can be described using models of similar form, i.e., a time evolution equation for a purely dissipative system without any inertia based on a gradient dynamics that is characterized by mobility functions and an underlying energy functional. Thereby the dynamics might have a non-conserved and/or conserved part. Equations, like the well known Cahn-Hilliard (purely conserved) and Allen-Cahn (purely non-conserved) equations represent limiting cases (with respect to the chosen dynamics) of this general evolution equation. They are normally used with a particularly simple form of the energy functional as well.

The three physical systems discussed here all fit into the general framework when chosing different mobilities and/or energy functionals. Beside the mathematical similarity the systems do as well model similar physical phenomena as the respective liquid and solid films structure under the influence of their effective interaction with the substrate. However, although most readers will agree that the epitaxial growth of quantum dots is a subject of surface science less of them might do so in the case of a dewetting liquid film. We hope that our review contributes to the development of a more unified view onto these processes of self-organisation at interfaces.

In particular, we have used two basic steps of mathematical analysis, namely the study of the linear stability of homogeneous steady states, i.e., flat films, and the mapping of non-trivial steady states, i.e., drop/hole (quantum dot) in dependence of system size for various values of interaction constants and/or mean film thickness. Our aim has been to illustrate that the underlying solution structure might be very complex as in the case of epitaxial growth but can be understood better when comparing to the much simpler results for the dewetting liquid film. We have furthermore shown that the continuation techniques employed can shed some light on this structure in a more convenient way than time-stepping methods. One might further argue that understanding the solution structure of the quantum-dot system might as well allow to predict pathways of evolution in time for an epitaxial layer as the behaviour will ultimately be determined by the steady solutions

and their stability. This procedure was already followed for thin liquid films [71, 74, 96].

The usage of a general formulation like Eq. (1) does not only relate seemingly not related physical systems mathematically. It does as well allow to discuss model extensions in a more unified way. Taking epitaxial growth as example, the general form (1) would propose that in the non-conserved case, i.e., when material is deposited from the gas phase continuously the non-conserved part of the equation should be $-M_{\rm nc}\delta F/\delta\phi$ with F given by (4). The constant depostion often used in the literature would then only refer to the limit of a rather large chemical potential. Oblique deposition of material [38] might as well be modelled incorporating beside the vertical influx as well lateral driving contributions.

The here reviewed formulation can be extended in a straightforward way to the case of N coupled fields $\boldsymbol{\phi} = (\phi_1, \phi_2, \ldots, \phi_N)$ following a gradient dynamics that is governed by an energy functional $F[\phi_1, \phi_2, \ldots, \phi_N]$. The evolution equation is

$$\partial_t \boldsymbol{\phi} \;=\; \nabla \cdot \left[\underline{\mathbf{M}}_{\rm c} \cdot \nabla \frac{\delta F}{\delta \boldsymbol{\phi}} \right] \;-\; \underline{\mathbf{M}}_{\rm nc} \cdot \frac{\delta F}{\delta \boldsymbol{\phi}} \tag{10}$$

with the $\underline{\mathbf{M}}_{\rm c}(\boldsymbol{\phi}) \geq 0$ and $\underline{\mathbf{M}}_{\rm nc}(\boldsymbol{\phi}) \geq 0$ being symmetric positive-definite mobility matrices for the conserved and non-conserved part of the dynamics, respectively. They are formed by $N \times N$ mobility functions, respectively. Note that $\delta F/\delta\boldsymbol{\phi}$ corresponds to a vector of dimension N. A typical example is the evolution of a dewetting two-layer system where the ϕ_1 and ϕ_2 correspond to the two film thicknesses, respectively. The formulation as a special case of (10) is derived from the Navier-Stokes equations in the two liquid layers and appropriate boundary conditions for spatially two- and three-dimensional settings in Refs. [96–99]. The formulation in the form of Eq. (10) has the advantage that one can easily check the consistencey of the mobility functions after a normally rather involved derivation. Furthermore one can draw on rather general results, e.g., for the linear stability of flat film solutions [97]. Note, that such a formulation will apply to any multi-layer system in a relaxational setting, including films of dielectric liquids in a capacitor [100, 101] or multilayer pending films under the influence of gravity. We expect it to hold as well for the relaxation dynamics of multilayer epitaxial films.

Let us finally note that we have entirely excluded spatially heterogeneous systems, i.e., systems described by equations of form (1) where the energy depends explicitly on position. Such systems are already treated for dewetting films [17, 71, 82, 102–104], however, we are not aware of any such studies for epitaxial growth. We have as well excluded laterally driven systems described by equations like (1) that additionally include lateral driving forces. A comparison of sliding

droplets on an incline [34, 88], a driven (or convective) Cahn-Hilliard system [79] and epitaxial growth under oblique deposition might be rather interesting, for instance, in terms of coarsening behaviour [34, 94, 105, 106]. The combination of both effects, i.e., heterogeneous systems with lateral driving allows to describe the depinning and stick-slip motion of droplets [92, 107]. The problems has up to now, however, no counterpart in epitaxial growth.

---

[1] N. Ghoniem and D. D. Walgraef, *Instabilities and Selforganisation in Materials* (Oxford University Press, Oxford, 2008).

[2] D. D. Vvedensky, J. Phys.-Condes. Matter **16**, R1537 (2004).

[3] J. S. Langer, in C. Godreche, ed., *Solids far from Equilibrium* (Cambridge University Press, 1992), pp. 297–363.

[4] J. W. Cahn and J. E. Hilliard, J. Chem. Phys. **28**, 258 (1958).

[5] J. W. Cahn, J. Chem. Phys. **42**, 93 (1965).

[6] P.-G. de Gennes, Rev. Mod. Phys. **57**, 827 (1985).

[7] J. N. Israelachvili, *Intermolecular and Surface Forces* (Academic Press, London, 1992).

[8] V. S. Mitlin, J. Colloid Interface Sci. **156**, 491 (1993).

[9] A. Oron, S. H. Davis, and S. G. Bankoff, Rev. Mod. Phys. **69**, 931 (1997).

[10] L. M. Pismen and Y. Pomeau, Phys. Rev. E **62**, 2480 (2000).

[11] S. Kalliadasis and U. Thiele, eds., *Thin Films of Soft Matter* (Springer, Wien / New York, 2007), ISBN 978-3-211-69807-5, CISM 490.

[12] R. Fetzer, K. Jacobs, A. Münch, B. Wagner, and T. P. Witelski, Phys. Rev. Lett. **95**, 127801 (2005).

[13] A. V. Lyushnin, A. A. Golovin, and L. M. Pismen, Phys. Rev. E **65**, 021602 (2002).

[14] J. P. Burelbach, S. G. Bankoff, and S. H. Davis, J. Fluid Mech. **195**, 463 (1988).

[15] A. Oron and S. G. Bankoff, J. Colloid Interface Sci. **218**, 152 (1999).

[16] L. W. Schwartz, R. V. Roy, R. R. Eley, and S. Petrash, J. Colloid Interface Sci. **214**, 363 (2001).

[17] K. Kargupta, R. Konnur, and A. Sharma, Langmuir **17**, 1294 (2001).

[18] M. Bestehorn and D. Merkt, Phys. Rev. Lett. **97**, 127802 (2006).

[19] I. E. Dzyaloshinskii, E. M. Lifshitz, and L. P. Pitaevskii, Sov. Phys. JETP **37**, 161 (1960).

[20] E. Ruckenstein and R. K. Jain, J. Chem. Soc. Faraday Trans. II **70**, 132 (1974).

[21] L. M. Hocking, Phys. Fluids A **5**, 793 (1993).

[22] A. Sharma and R. Khanna, Phys. Rev. Lett. **81**, 3463 (1998).

[23] M. H. Eres, L. W. Schwartz, and R. V. Roy, Phys. Fluids **12**, 1278 (2000).

[24] U. Thiele, M. G. Velarde, K. Neuffer, and Y. Pomeau, Phys. Rev. E **64**, 031602 (2001).

[25] Z. Lin, T. Kerle, S. M. Baker, D. A. Hoagland, E. Schäffer, U. Steiner, and T. P. Russell, J. Chem. Phys. **114**, 2377 (2001).

[26] Z. Lin, T. Kerle, T. P. Russell, E. Schäffer, and U. Steiner, Macromolecules **35**, 3971 (2002).

[27] R. Verma, A. Sharma, K. Kargupta, and J. Bhaumik, Langmuir **21**, 3710 (2005).

[28] K. John and U. Thiele, Appl. Phys. Lett. **90**, 264102 (2007).

[29] K. John, P. Hänggi, and U. Thiele, Soft Matter **4**, 1183 (2008).

[30] A. Oron and P. Rosenau, J. Fluid Mech. **273**, 361 (1994).

[31] A. A. Golovin, A. A. Nepomnyashchy, and L. M. Pismen, Phys. Fluids **6**, 34 (1994).

[32] A. Oron, Phys. Rev. Lett. **85**, 2108 (2000).

[33] M. Bestehorn, A. Pototsky, and U. Thiele, Eur. Phys. J. B **33**, 457 (2003).

[34] U. Thiele and E. Knobloch, Physica D **190**, 213 (2004).

[35] D. Merkt, A. Pototsky, M. Bestehorn, and U. Thiele, Phys. Fluids **17**, 064104 (2005).

[36] A. Novick-Cohen and L. A. Segel, Physica D **10**, 277 (1984).

[37] L. Frastia, L. Pismen, and U. Thiele, (submitted).

[38] B. J. Spencer, P. W. Voorhees, and S. H. Davis, Phys. Rev. Lett. **67**, 3696 (1991).

[39] T. V. Savina, A. A. Golovin, S. H. Davis, A. A. Nepomnyashchy, and P. W. Voorhees, Phys. Rev. E **67**, 021606 (2003).

[40] A. A. Golovin, M. S. Levine, T. V. Savina, and S. H. Davis, Phys. Rev. B **70**, 235342 (2004).

[41] A. A. Golovin, S. H. Davis, and A. A. Nepomnyashchy, Phys. Rev. E **59**, 803 (1999).

[42] M. Siegert, Physica A **239**, 420 (1997).

[43] M. Haataja, J. Muller, A. D. Rutenberg, and M. Grant, Phys. Rev. B **65**, 165414 (2002).

[44] Y. Y. Pang and R. Huang, Phys. Rev. B **74**, 075413 (2006).

[45] Y. Y. Pang and R. Huang, J. Appl. Phys. **101**, 023519 (2007).

[46] W. T. Tekalign and B. J. Spencer, J. Appl. Phys. **102**, 073503 (2007).

[47] E. Doedel, H. B. Keller, and J. P. Kernevez, Int. J. Bifurcation Chaos **1**, 493 (1991).

[48] E. Doedel, H. B. Keller, and J. P. Kernevez, Int. J. Bifurcation Chaos **1**, 745 (1991).

[49] E. J. Doedel, A. R. Champneys, T. F. Fairgrieve, Y. A. Kuznetsov, B. Sandstede, and X. J. Wang, *AUTO97: Continuation and bifurcation software for ordinary differential equations* (Concordia Uni-

versity, Montreal, 1997).

[50] P. Beltrame and U. Thiele, (submitted).

[51] D. M. Anderson, G. B. McFadden, and A. A. Wheeler, Ann. Rev. Fluid Mech. **30**, 139 (1998).

[52] S. M. Wise, J. S. Lowengrub, J. S. Kim, and W. C. Johnson, Superlattices Microstruct. **36**, 293 (2004).

[53] E. Rabani, D. R. Reichman, P. L. Geissler, and L. E. Brus, Nature **426**, 271 (2003).

[54] G. Yosef and E. Rabani, J. Phys. Chem. B **110**, 20965 (2006).

[55] I. Vancea, U. Thiele, E. Pauliac-Vaujour, A. Stannard, C. P. Martin, M. O. Blunt, and P. J. Moriarty, Phys. Rev. E **78**, 041601 (2008).

[56] T. Vicsek, *Fractal Growth Phenomena* (World Scientific, Singapore, 1989), 1st ed.

[57] H. Hinrichsen, Physica A **369**, 1 (2006).

[58] G. Reiter, Phys. Rev. Lett. **68**, 75 (1992).

[59] R. Seemann, S. Herminghaus, C. Neto, S. Schlagowski, D. Podzimek, R. Konrad, H. Mantz, and K. Jacobs, J. Phys.-Condes. Matter **17**, S267 (2005).

[60] U. Thiele, M. Mertig, and W. Pompe, Phys. Rev. Lett. **80**, 2869 (1998).

[61] C. P. Martin, M. O. Blunt, E. Pauliac-Vaujour, A. Stannard, P. Moriarty, I. Vancea, and U. Thiele, Phys. Rev. Lett. **99**, 116103 (2007).

[62] L. M. Pismen, Phys. Rev. E **6402**, 021603 (2001).

[63] L. M. Pismen and Y. Pomeau, Phys. Fluids **16**, 2604 (2004).

[64] L. M. Pismen and U. Thiele, Phys. Fluids **18**, 042104 (2006).

[65] U. Thiele, M. G. Velarde, K. Neuffer, M. Bestehorn, and Y. Pomeau, Phys. Rev. E **64**, 061601 (2001).

[66] G. F. Teletzke, H. T. Davis, and L. E. Scriven, Rev. Phys. Appl. **23**, 989 (1988).

[67] A. Oron and P. Rosenau, J. Physique II France **2**, 131 (1992).

[68] A. Sharma, Langmuir **9**, 3580 (1993).

[69] A. Sharma and G. Reiter, J. Colloid Interface Sci. **178**, 383 (1996).

[70] U. Thiele, K. Neuffer, Y. Pomeau, and M. G. Velarde, Colloid Surf. A **206**, 135 (2002).

[71] U. Thiele, L. Brusch, M. Bestehorn, and M. Bär, Eur. Phys. J. E **11**, 255 (2003).

[72] K. John, M. Bär, and U. Thiele, Eur. Phys. J. E **18**, 183 (2005).

[73] U. Thiele, J. M. Vega, and E. Knobloch, J. Fluid Mech. **546**, 61 (2006).

[74] U. Thiele, M. G. Velarde, and K. Neuffer, Phys. Rev. Lett. **87**, 016104 (2001).

[75] J. Becker, G. Grün, R. Seemann, H. Mantz, K. Jacobs, K. R. Mecke, and R. Blossey, Nat. Mater. **2**,

59 (2003).

[76] U. Thiele, Eur. Phys. J. E **12**, 409 (2003).

[77] J. A. Diez and L. Kondic, Phys. Fluids **19**, 072107 (2007).

[78] P. Beltrame, P. Hänggi, and U. Thiele, (submitted).

[79] A. A. Golovin, A. A. Nepomnyashchy, S. H. Davis, and M. A. Zaks, Phys. Rev. Lett. **86**, 1550 (2001).

[80] U. Thiele, S. Madruga, and L. Frastia, Phys. Fluids **19**, 122106 (2007).

[81] A. L. Bertozzi, G. Grün, and T. P. Witelski, Nonlinearity **14**, 1569 (2001).

[82] L. Brusch, H. Kühne, U. Thiele, and M. Bär, Phys. Rev. E **66**, 011602 (2002).

[83] K. B. Glaser and T. P. Witelski, Phys. Rev. E **67**, 016302 (2003).

[84] K. B. Glasner and T. P. Witelski, Physica D **209**, 80 (2005).

[85] A. Torcini and P. Politi, Eur. Phys. J. B **25**, 519 (2002).

[86] R. V. Kohn and F. Otto, Commun. Math. Phys. **229**, 375 (2002).

[87] M. Bestehorn and K. Neuffer, Phys. Rev. Lett. **87**, 046101 (2001).

[88] U. Thiele, K. Neuffer, M. Bestehorn, Y. Pomeau, and M. G. Velarde, Colloid Surf. A **206**, 87 (2002).

[89] A. Pereira, P. M. J. Trevelyan, U. Thiele, and S. Kalliadasis, Phys. Fluids **19**, 112102 (2007).

[90] U. Thiele and E. Knobloch, Phys. Fluids **15**, 892 (2003).

[91] B. Scheid, C. Ruyer-Quil, U. Thiele, O. A. Kabov, J. C. Legros, and P. Colinet, J. Fluid Mech. **527**, 303 (2005).

[92] U. Thiele and E. Knobloch, New J. Phys. **8**, 313, 1 (2006).

[93] M. Siegert, Phys. Rev. Lett. **81**, 5481 (1998).

[94] S. J. Watson and S. A. Norris, Phys. Rev. Lett. **96**, 176103 (2006).

[95] P. H. Leo and W. C. Johnson, Acta Mater. **49**, 1771 (2001).

[96] A. Pototsky, M. Bestehorn, D. Merkt, and U. Thiele, Phys. Rev. E **70**, 025201(R) (2004).

[97] A. Pototsky, M. Bestehorn, D. Merkt, and U. Thiele, J. Chem. Phys. **122**, 224711 (2005).

[98] L. S. Fisher and A. A. Golovin, J. Colloid Interface Sci. **291**, 515 (2005).

[99] A. Pototsky, M. Bestehorn, D. Merkt, and U. Thiele, Europhys. Lett. **74**, 665 (2006).

[100] D. Bandyopadhyay, R. Gulabani, and A. Sharma, Ind. Eng. Chem. Res. **44**, 1259 (2005).

[101] D. Bandyopadhyay and A. Sharma, J. Colloid Interface Sci. **311**, 595 (2007).

[102] P. Lenz and R. Lipowsky, Phys. Rev. Lett. **80**, 1920 (1998).

[103] C. Bauer, S. Dietrich, and A. O. Parry, Europhys. Lett. **47**, 474 (1999).

[104] R. Konnur, K. Kargupta, and A. Sharma, Phys. Rev. Lett. **84**, 931 (2000).

[105] C. L. Emmott and A. J. Bray, Phys. Rev. E **54**, 4568 (1996).

[106] S. J. Watson, F. Otto, B. Y. Rubinstein, and S. H. Davis, Physica D **178**, 127 (2003).

[107] U. Thiele and E. Knobloch, Phys. Rev. Lett. **97**, 204501 (2006).